Numerical Study on the Jet Dynamic through Centrifuge Spinning: Influence of Angular Velocity

Afsaneh Valipouri, Seyed Abdolkarim Hosseini Ravandi, Ahmadreza Pishevar and Emilian I Părău

Abstract—**Centrifuge spinning is a method that makes possible of fabrication nanofibers rapidly and at high yields. In the centrifugal spinning process, a polymer solution is delivered by the centrifugal force through small nozzle of a rapidly rotating cylindrical drum. Thereby, thin fibers are formed and collected on a collector in the form of a web. In this study, a mathematical model of the dynamics of a viscous liquid jet, which emerges from rotating drum through centrifuge spinning, was derived. The Navier-Stokes equations were solved in this system with the usual viscous free surface boundary conditions. One-dimensional equations were derived using asymptotic methods based upon a slender jet assumption and solved numerically. The effect of angular velocity upon the trajectory, radius, and tangential velocity of the jet was simulated and presented. Increasing angular velocity resulted in a decrease in the size of the liquid jet. Also, increasing angular velocity tended to increase the jet velocity which translated to increase the production rate. The jet centerline became more tightly coiled when the angular velocity increased. In addition, simulated jet diameter was compared with some results reported in our previous work.**

Keywords: Centrifuge spinning, Navier-Stokes equations, curved jet, angular velocity.

I. INTRODUCTION

When the diameter of the fibers are in the nanometer range, several amazing characteristics appear, such as very large surface area to volume ratio, flexibility in surface functionalities, and superior mechanical performance (e.g. stiffness and tensile strength) compared with any other known form of material [1]. The unique properties of nanofibers make them favorable for many applications such as tissue engineering scaffolds [2,3], filtration devices [4-6], sensors [7,8], materials development [9], and electronic applications [10]. There are several methods for fabrication of nanofibers [11-13]. Electrospinning is an effective and versatile technique used to prepare nanofibers[14-16].

The challenge associated with electrospinning is its production rate. The relatively low production rate of a traditional electrospinning has limited the industrial applications of this system [17]. A few methods for producing electrospun nanofibers at higher mass production rate are suggested. For instance, modified single-needle [18,19], multi-needle [20-28], needleless systems [29-35] and a plastic filter set-up [36] have been developed to enhance nanofiber production rate. A newly developed method of producing nanofibers, called forcespinning, has proven to be a viable alternative to mass produce nanofibers. Also, attempt has been made to enhance the production rate of nanofibers with the development of electro-mechanical system. Some researchers have combined centrifugal forces from a rotating disk with electrostatic forces to fabricate nano-scale fibers [37,38]. The previous research has indicated that applying the centrifugal force results in a significant increase in the production rate of nanofibers [39-41].

In the centrifuge spinning or forcespinning, a polymer solution sustained by its surface tension is radially transported outward through the nozzle by the centrifugal force. Further increase of the rotational speed of spinning head results in a critical value by which the centrifugal force overcomes the surface tension and the jet of the fluid is ejected from the tip of the nozzle. The centrifugal force directs the liquid jet toward the collector and stretches the jet to become very fine [42]. The traveling jet is solidified through solvent evaporation and the solidified jet, turning into the nanofibers, is collected in the form of nanofiber mat on the metallic cylindrical collector. The important parameters involved in fabrication process through centrifuge spinning include: spinneret angular velocity and orifice radius, polymer viscoelasticity (which includes viscosity and relaxation time of the material), surface tension, evaporation rate (for solvent in solution) and temperature (melting and solidification), and distance of spinneret orifice to collector.

For the centrifuge spinning method, large deformations are experienced in a short period of time, in which case non-linear models must be used to simulate the jet dynamic.

In this study, firstly the centrifuge spinning is developed to be isolated from air ambient. Secondly, we have introduced three-dimensional equations of the curved jet through air-sealed centrifuge spinning. Also, the equations are solved by finite difference method. Finally, the effect of angular velocity is theoretically investigated and discussed. Also, a comparison is drawn between theoretical predictions and previously reported experimental data.

A. *Air-sealed centrifuge spinning*

As Fig. 1 shows, the air-sealed centrifuge spinning setup consists of a rotating drive shaft (A), an insulated plate (B),

A. Valipouri and S. A. Hosseini Ravandi are with the Department of Textile Engineering and A. Pishevar is with the Department of Mechanical Engineering of Isfahan University of Technology, Isfahan, Iran. E. I. Părău is with the School of Mathematics, University of East Anglia UEA, Norwich, UK. Correspondence should be addressed to S. A. Hosseini Ravandi (e-mail: hoseinir@cc.iut.ac.ir).

a rotating cylindrical receptacle (C), a metallic cylindrical collector (D), and a transparent door (E). The rotating cylindrical receptacle holds a syringe containing polymer solution with a needle attached to the syringe. Polymer solution is ejected from the needle tip. The receptacle and the collector are firmly affixed to the drive shaft by the plate. The movable transparent door is used to prevent air from entering and exiting.

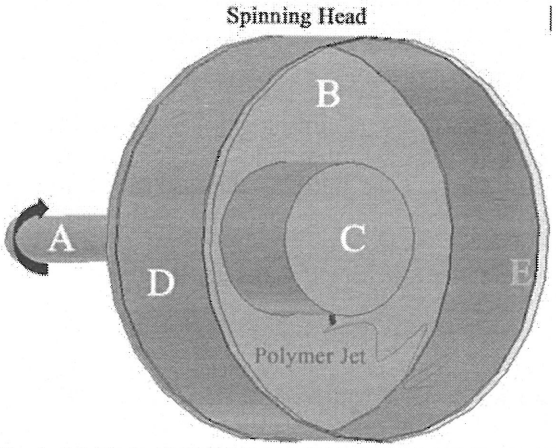

Fig. 1. Schematic of air-sealed centrifuge spinning system, (A) rotating drive shaft (B) insulated plate (C) rotating cylindrical receptacle (D) rotating metallic cylindrical collector (E) transparent door.

The collection of the receptacle, the nozzle, the collector, the insulated plate, and the transparent door is called spinning head. As the spinning head accelerates, a pendant drop originates from the orifice due to the centrifugal forces experienced on the fluid within the nozzle. The centrifugal force directs the liquid jet toward the collector and stretches the jet to become very fine. The traveling jet is solidified through solvent evaporation and the solidified jet, turning into the nanofiber, is collected in the form of nanofiber mat on the metallic cylindrical collector.

II. MODELING PROCEDURE

A. *Governing equations*

Air-sealed centrifuge spinning process contains 3D Navier-Stokes and continuity equations for a curved liquid jet in the inviscid and viscous cases, namely.

$$\nabla.\vec{u} = 0 \tag{1}$$

and

$$\frac{\partial\vec{u}}{\partial t} + (\vec{u}\,.\,\nabla)\vec{u} = -\frac{1}{\rho}\nabla p + \frac{\mu}{\rho}\nabla^2\vec{u} - 2\vec{\omega}\times\vec{u} - \vec{\omega}\times(\vec{\omega}\times\vec{r}) \tag{2}$$

The components of the Navier-Stokes equations include the local acceleration, the convective acceleration, the acceleration due to pressure, Coriolis acceleration, and centrifugal acceleration, in order from left to right.

The radius of the nozzle which situated on the curved face of a cylindrical drum of radius s_0, is described by a. Cylindrical drum is rotating on its axis at a constant rate of Ω. The coordinate system used was an extension to cylindrical polar coordinates, (s, n, φ), where s is the arc-length along the jet and (n, φ) is polar coordinate in any cross section of the jet. The radius of the fiber is described by R. This system was established and shown in more detail by Wallwork *et al.* [43,44].

B. *Non-dimensionalization of governing equations*

The governing equations are converted to dimensionless form using the following characteristic scales and dimensionless groups

Characteristic Scales

Tangential velocity: $\bar{u} = \frac{u}{U}$

Radial velocity: $\bar{v} = \frac{v}{U}$

Azimuthal velocity: $\bar{\omega} = \frac{\omega}{U}$

Pressure: $\bar{p} = \frac{p}{\rho U^2}$

Radial point between the center and surface of the jet: $\bar{n} = \frac{n}{a}$

Radius of the jet: $\bar{R} = \frac{R}{a}$

Time: $\bar{t} = \frac{tU}{s_0}$

Arc-length coordinates: $\bar{X} = \frac{X}{s_0}$ and $\bar{Z} = \frac{Z}{s_0}$

Aspect ratio: $\epsilon = \frac{a}{s_0}$

Dimensionless Groups

Reynolds number: $\mathrm{Re} = \frac{\rho U a}{\mu}$

Rossby number: $\mathrm{Rb} = \frac{U}{s_0\Omega}$

Weber number: $\mathrm{We} = \frac{\rho U^2 a}{\gamma}$

Using these dimensionless groups into the continuity and Navier-Stokes equations regarding to curvilinear coordinate gives the following dimensionless governing equations (overbars are dropped).

Dimensionless continuity equation:

$$\epsilon n\frac{\partial u}{\partial s} + \left(1 + \epsilon n\cos\varphi(X_sZ_{ss} - Z_sX_{ss})\right)\left[v + n\frac{\partial v}{\partial n} + \frac{\partial\omega}{\partial\varphi}\right] + \epsilon n(X_sZ_{ss} - Z_sX_{ss})(v\cos\varphi - \omega\sin\varphi) = 0 \tag{3}$$

$\mathbf{e}_s$ component of Navier–Stokes equation:

$$h_s\left(\epsilon\frac{\partial u}{\partial t} + \epsilon(v\cos\varphi - \omega\sin\varphi)(Z_{st}X_s - X_{st}Z_s) + v\frac{\partial u}{\partial n} + \frac{w}{n}\frac{\partial u}{\partial\varphi}\right)$$
$$+\epsilon u\frac{\partial u}{\partial s} + \epsilon u(X_sZ_{ss} - X_{ss}Z_s)(v\cos\varphi - \omega\sin\varphi) =$$
$$-\epsilon\frac{\partial p}{\partial s} + \left(\frac{2}{\mathrm{Rb}}\epsilon(v\cos\varphi - \omega\sin\varphi) + \frac{\epsilon}{\mathrm{Rb}^2}\left((X+1)X_s + ZZ_s\right)\right)h_s$$
$$+\frac{1}{\mathrm{Re}}\frac{1}{n\epsilon}\left\{\frac{-\epsilon^3n^2\cos\varphi(X_sZ_{sss} - Z_sX_{sss})}{h_s^2}\left(\frac{\partial u}{\partial s} + (v\cos\varphi - \omega\sin\varphi)(X_sZ_{ss} - Z_sX_{ss})\right)\right.$$
$$+\frac{\epsilon^2n}{h_s}\left(-u(X_sZ_{ss} - Z_sX_{ss})^2 + \frac{\partial u^2}{\partial s^2} + 2\frac{\partial v}{\partial s}\cos\varphi(X_sZ_{ss} - Z_sX_{ss}) + v\cos\varphi(X_sZ_{sss} - Z_sX_{sss})\right.$$
$$\left.\left.-2\frac{\partial\omega}{\partial s}\sin\varphi(X_sZ_{ss} - Z_sX_{ss}) - \omega\sin\varphi(X_sZ_{sss} - Z_sX_{sss})\right)\right.$$

$$+(1+2\epsilon n\cos\varphi(X_sZ_{ss}-Z_sX_{ss}))\frac{\partial u}{\partial n}$$
$$+nh_s\frac{\partial^2 u}{\partial n^2}-\epsilon\frac{\partial u}{\partial\varphi}\sin\varphi(X_sZ_{ss}-Z_sX_{ss})+\frac{h_s}{n}\frac{\partial^2 u}{\partial\varphi^2}\}$$

(4)

$\mathbf{e_n}$ component of Navier–Stokes equation:

$$h_s\left(\epsilon\frac{\partial v}{\partial t}+\epsilon u\cos\varphi(X_{st}Z_s-Z_{st}X_s)+v\frac{\partial v}{\partial n}+\frac{\omega}{n}\frac{\partial v}{\partial\varphi}-\frac{\omega^2}{n}\right)$$
$$+\epsilon u\frac{\partial v}{\partial s}-\epsilon u^2\cos\varphi(X_sZ_{ss}-Z_sX_{ss})$$
$$=(-\frac{\partial p}{\partial n}-\frac{2\epsilon}{Rb}u\cos\varphi$$
$$+\epsilon\frac{\cos\varphi}{Rb^2}((X+1)Z_s-ZX_s$$
$$+\epsilon n\cos\varphi))h_s$$
$$+\frac{1}{Re}\frac{1}{\epsilon n}\{\frac{-\epsilon^3n^2\cos\varphi(X_sZ_{sss}-Z_sX_{sss})}{h_s^2}(\frac{\partial v}{\partial s}$$
$$-u\cos\varphi(X_sZ_{ss}-Z_sX_{ss}))$$
$$+\frac{\epsilon^2 n}{h_s}\left(-v\cos^2\varphi(X_sZ_{ss}-Z_sX_{ss})^2+\frac{\partial^2 v}{\partial s^2}\right.$$
$$-2\frac{\partial u}{\partial s}\cos\varphi(X_sZ_{ss}-Z_sX_{ss})$$
$$-u\cos\varphi(X_sZ_{sss}-Z_sX_{sss})$$
$$\left.+\omega\sin\varphi\cos\varphi(X_sZ_{ss}-Z_sX_{ss})^2\right)$$
$$+(1+2\epsilon n\cos\varphi(X_sZ_{ss}-Z_sX_{ss}))\frac{\partial v}{\partial n}+nh_s\frac{\partial^2 v}{\partial n^2}-\epsilon(\frac{\partial v}{\partial\varphi}$$
$$-\omega)\sin\varphi(X_sZ_{ss}-Z_sX_{ss})$$
$$+\frac{h_s}{n}(\frac{\partial^2 v}{\partial\varphi^2}-v-2\frac{\partial\omega}{\partial\varphi})\}$$

(5)

$\mathbf{e_\varphi}$ component of Navier–Stokes equation:

$$h_s\left(\epsilon\frac{\partial\omega}{\partial t}+\epsilon u\sin\varphi(Z_{st}X_s-X_{st}Z_s)+v\frac{\partial\omega}{\partial n}+\frac{\omega}{n}\frac{\partial\omega}{\partial\varphi}\right.$$
$$\left.+\frac{v\omega}{n}\right)+\epsilon u\frac{\partial\omega}{\partial s}$$
$$+\epsilon\sin\varphi(X_sZ_{ss}-Z_sX_{ss})u^2$$
$$=(-\frac{1}{n}\frac{\partial p}{\partial\varphi}+\frac{2\epsilon}{Rb}u\sin\varphi$$
$$+\frac{\epsilon}{Rb^2}\sin\varphi(ZX_s-(X+1)Z_s$$
$$-\epsilon n\cos\varphi))h_s$$
$$+\frac{1}{Re}\frac{1}{\epsilon n}\{\frac{-\epsilon^3n^2\cos\varphi(X_sZ_{sss}-Z_sX_{sss})}{h_s^2}(\frac{\partial\omega}{\partial s}$$
$$+u\sin\varphi(X_sZ_{ss}-Z_sX_{ss}))$$
$$+\frac{\epsilon^2 n}{h_s}\left(-\omega\sin^2\varphi(X_sZ_{ss}-Z_sX_{ss})^2+\frac{\partial^2\omega}{\partial s^2}\right.$$
$$+2\frac{\partial u}{\partial s}\sin\varphi(X_sZ_{ss}-Z_sX_{ss})$$
$$+u\sin\varphi(X_sZ_{sss}-X_{sss}Z_s)$$
$$\left.+v\sin\varphi\cos\varphi(X_sZ_{ss}-Z_sX_{ss})^2\right)$$
$$+(1+2\epsilon n\cos\varphi(X_sZ_{ss}-Z_sX_{ss}))\frac{\partial\omega}{\partial n}+nh_s\frac{\partial^2\omega}{\partial n^2}-\epsilon(\frac{\partial\omega}{\partial\varphi}$$
$$+v)\sin\varphi(X_sZ_{ss}-Z_sX_{ss})$$
$$+\frac{h_s}{n}(\frac{\partial^2\omega}{\partial\varphi^2}-\omega+2\frac{\partial v}{\partial\varphi})\}$$

(6)

Where

$$E'=\left(1+\epsilon^2\frac{1}{h_s^2}\left(\frac{\partial R}{\partial s}\right)^2+\frac{1}{n^2}\left(\frac{\partial R}{\partial\varphi}\right)^2\right)^{\frac{1}{2}}$$

(7)

$$h_s=1+\epsilon n\cos\varphi\left(X_sZ_{ss}-Z_sX_{ss}\right)$$

[45]

Where u is the velocity of the jet, p is the pressure, ρ is the density, ω is the angular velocity, r is the position vector in the rotating frame, μ is the viscosity, and t is the time.

C. *Asymptotic analysis*

These equations are difficult in general to be solved, but the slenderness of the fluid geometry enables the simplification of the full three-dimensional mathematical model by means of asymptotic analysis. The variables are expanded as follows:

$$u=u_0(s,t)+(\epsilon n)u_1(s,\varphi,t)+(\epsilon n)^2u_2(s,\varphi,t)+\cdots$$
$$v=(\epsilon n)v_1(s,\varphi,t)+(\epsilon n)^2v_2(s,\varphi,t)+\cdots$$
$$w=(\epsilon n)w_1(s,\varphi,t)+(\epsilon n)^2w_2(s,\varphi,t)+\cdots$$
$$p=p_0(s,\varphi,t)+(\epsilon n)p_1(s,\varphi,t)+(\epsilon n)^2p_2(s,\varphi,t)+\cdots \quad (8)$$
$$R=R_0(s,t)+(\epsilon)R_1(s,\varphi,t)+(\epsilon)^2R_2(s,\varphi,t)+\cdots$$
$$X=X_0(s)+(\epsilon)X_1(s,t)+(\epsilon)^2X_2(s,t)+\cdots$$
$$Z=Z_0(s)+(\epsilon)Z_1(s,t)+(\epsilon)^2Z_2(s,t)+\cdots$$

D. *Steady state solutions*

One-dimensional equations were derived by assumption that the flow is uniaxial and the center-line of the jet is steady at the leading order and it does not depend on time.

$$(X_sZ_{ss}-X_{ss}Z_s)(u_0^2-\frac{3}{Re}u_{0s}-\frac{1}{WeR_0})-\frac{2}{Rb}u_0$$
$$+\frac{(X+1)Z_s-ZX_s}{Rb^2}=0 \quad (9)$$

$$u_0u_{0s}=-\frac{1}{We}(\frac{1}{R_0})_s+\frac{ZZ+(X+1)X_s}{Rb^2}+\frac{3(R_0^2u_{0s})_s}{ReR_0^2} \quad (10)$$

$$\frac{u_{0s}}{2}R_0+u_0R_{0s}=0 \quad (11)$$

$$X_s^2+Z_s^2=1 \quad (12)$$

It can be observed from Eq. 11 that $R_0^2u_0$ is constant and, by using $R_0(0)=1$ and $u_0(0)=1$, we have $R_0^2u_0=1$, therefore R_0 can be replaced by $1/\sqrt{u_0}$,

$$(X_sZ_{ss}-X_{ss}Z_s)(u_0^2-\frac{3}{Re}u_{0s}-\frac{\sqrt{u_0}}{We})-\frac{2}{Rb}u_0$$
$$+\frac{(X+1)Z_s-ZX_s}{Rb^2}=0 \quad (13)$$

$$u_0u_{0s}=-\frac{1}{We}\frac{u_{0s}}{2\sqrt{u_0}}+\frac{ZZ+(X+1)X_s}{Rb^2}$$
$$+\frac{3}{Re}(u_{0ss}-\frac{u_{0s}^2}{u_0}) \quad (14)$$

$$X_s^2+Z_s^2=1 \quad (15)$$

[45]

E. Boundary conditions

The boundary conditions at the nozzle are $X(0)=Z(0)=Z_s(0)=0, u_0(0)=X_s(0)=1$.

F. Numerical solution of the problem

The final problem consists of three unknown variables namely X_s, Z_s and u_0 in fact and the values of X and Z are obtained by trapezoidal-rule integration. In order to solve the problem, a good initial guess must be provided for each solution step. The first initial guess required to get started was taken as a straight cylinder of constant radius, without rotation. The nonlinear equations (Eqs. 13, 14 and 15) are solved at each step using Newton's method. The previously calculated solution was used to provide initial guess for the next step.

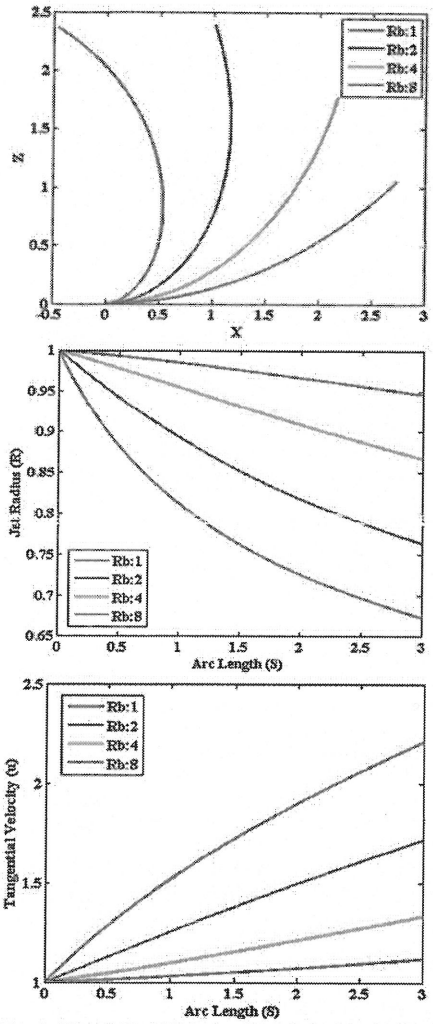

Fig. 2. Upper: Jet trajectory, Center: Jet radius versus arc length, Bottom: Tangential velocity versus arc length with varying Rossby numbers, We=100, Re=4.

III. RESULTS AND DISCUSSION

A. Simulation results

In provided model, there are three non-dimensional numbers, the Weber (We), Rossby (Rb), and Reynolds (Re) numbers, defined as: $\mathrm{Re}=\frac{\rho U a}{\mu}$, $\mathrm{Rb}=\frac{U}{s_0\Omega}$, $\mathrm{We}=\frac{\rho U^2 a}{\gamma}$, where u is the velocity of the jet, ρ is the density, Ω is the angular velocity, μ is the viscosity, γ is the surface tension, s_0 is radius of cylindrical drum, and a is the nozzle radius.

The influence of the Rossby number on jet trajectory, jet diameter, and tangential velocity of the jet is shown in Fig. 2. Increasing the angular velocity decreases Rossby number. The trajectory plot shows that with decreasing Rossby number while keeping We and Re constant at 100 and 4, respectively, the jet path becomes more tightly coiled, getting closer to the center of rotation. It can be seen from middle plot of Fig. 2 that as the Rossby number increases, the fiber radius increases. Decreasing Rossby number (increasing angular velocity) results in increasing fiber fineness. In fact, the centrifugal force is increased significantly by increasing the angular velocity. The centrifugal force accelerates and stretches the jet. Thus, the higher the centrifugal force, the greater the extension of polymeric jet, which results in thinner fiber diameters. Increasing the Rossby number also reduces the tangential velocity of the jet which translates to a lower production rate.

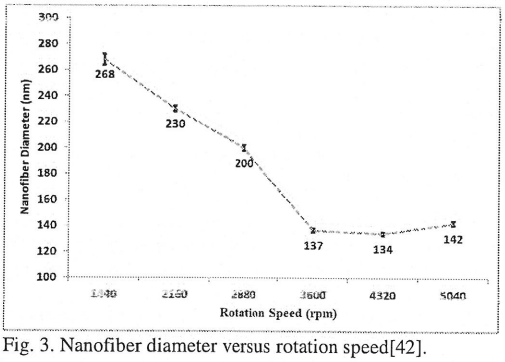

Fig. 3. Nanofiber diameter versus rotation speed[42].

B. Experimental validation

It has been found from our previous work [42] that the average diameter and standard deviation of nanofibers tended to decrease drastically with increasing the rotation speed from 1440 to 5040 rpm as shown in Fig. 3. In fact, the centrifugal force is increased significantly by increasing the speed of rotation (see Table I). As previously indicated, the centrifugal force accelerates and stretches the liquid jet. Thus, the higher the centrifugal force, the greater the extension of polymeric jet, which results in thinner fiber diameters. In addition, as the rotation speed is increased, there is a corresponding increase in the flow rate as indicated in Table I. Therefore, higher flow rate leads to increase in production rate.

TABLE I
THE RELATIONSHIP BETWEEN ROTATION SPEED, FLOW RATE AND CENTRIFUGAL FORCE [42]

Speed (rpm)	Centrifugal Force*	Flow rate (ml/h)
1440	980	0.0803
2160	2205	0.2862
2880	3921	0.5724
3600	6126	0.7111
4320	8822	0.9598
5040	12008	1.1346

$F_{cent}=\rho\omega^2 r$, ρ=0.863 g/cm^3, $\omega=2\pi$ rpm /60(rad/sec), r =0.05 m

Further increase of the rotation speed from 3600 rpm up to 5040 rpm did not lead to any significant difference in nanofibers diameter. There is a possible reason for this observation, i.e. spinning distance is a parameter which limits more extension of the jet. This parameter is constant through current work. A longer distance is needed by increasing the flow rate to obtain finer nanofibers. These findings confirm the simulation results.

IV. Conclusion

In order to simulate the jet dynamic, the Navier–Stokes equations were solved through centrifugal spinning system with the usual viscous free-surface boundary conditions, using an asymptotic method based upon a slender-jet assumption. The influence of the Rossby number showed that decreasing the Rossby number which can be translated to an increase in angular velocity, reduced the overall size of the fiber radius, contracted the trajectory, and increased the tangential velocity.

Therefore, the diameters of fibers could be manipulated by adjusting the angular velocity of the spinning head. Also, increasing the rotational speed results in an increasing in production rate of nanofibers. Finally, the experimental results were compared to numerical solutions of the Navier–Stokes equations. Some qualitative agreement was observed.

References

[1] Z. M. Huang, Y. Z. Zhang, M. Kotaki and S. A. Ramakrishna, "Review on polymer nanofibers by electrospinning and their applications in nanocomposites", *Compos. Sci. Technol.*, vol. 63, no. 15, pp. 2223–2253, 2003.

[2] M. P. Prabhakaran, J. Venugopal, C. K. Chan and S. Ramakrishna, "Surface modified electrospun nanofibrous scaffolds for nerve tissue engineering", *Nanotechnology*, vol. 19, no. 45, pp. 455102-455109, 2008.

[3] S. G. Kumbar, R. James, S. P. Nukavarapu and C. T. Laurencin, "Electrospun nanofiber scaffolds: Engineering soft tissues", *Biomed Mater*, vol. 3, no. 3, pp. 1-15, 2008.

[4] C. H. Hung and W. W. F. Leung, "Filtration of nano-aerosol using nanofiber filter under low Peclet number and transitional flow regime", *Sep. Purif. Technol.*, vol. 79, no. 1, pp. 34-42, 2011.

[5] Q. Zhang, J. Welch, H. Park, C-Y Wu, W. Sigmund and J. C. M. Marijnissen, "Improvement in nanofiber filtration by multiple thin layers of nanofiber mats", *J. Aerosol Sci.*, vol. 41, no. 2, pp. 230-236, 2010.

[6] D. Bjorge, N. Daels, S. D. Vrieze, P. Dejans, T. V. Camp, W. Audenaert, J. Hogie, P. Westbroek, K. De Clerck and S. W. H. Van Hulle, "Performance assessment of electrospun nanofibers for filter applications", *Desalination*, vol. 249, no. 3, pp. 942-948, 2009.

[7] D. Aussawasathien, J. H. Dong and L. Dai, "Electrospun polymer nanofiber sensors", *Synth. Met.*, vol. 154, no. 1-3, pp. 37-40, 2005.

[8] B. Ding, M. Wang, J. Yu and G. Sun, "Gas sensors based on electrospun nanofibers", *Sensors*, vol. 9, no. 3, pp. 1609-1624, 2009.

[9] J. S. Kim and D. H. Reneker, "Mechanical properties of composites using ultrafine electrospun fibers", *Polym. Composite.*, vol. 20, no. 1, pp. 124-131, 1999.

[10] Z. Rui, J. Chang-Yun, L. Xi-Zhe, L. Bin, K. Abhishek and S. Ramakrishna, "Improved adhesion of interconnected TiO2 nanofiber network on conductive substrate and its application in polymer photovoltaic devices", *Appl. Phys. Lett.*, vol. 93, no. 1, pp. 013102-013103, 2008.

[11] T. Ondarcuhu and C. Joachim, "Drawing a single nanofibre over hundreds of microns", *Europhys. Lett.*, vol. 42, no. 2, pp. 215-220, 1998.

[12] L. Feng, S. Li, H. Li, J. Zhai, Y. Song, L. Jiang and D. Zhu, "Super-hydrophobic surface of aligned polyacrylonitrile nanofibers", *Angew. Chem. Int. Ed. Engl.*, vol. 41, no. 7, pp. 1212-1223, 2002.

[13] G. M. Whitesides and B. Grzybowski, "Self-assembly at all scales", *Science*, vol. 295, no. 5564, pp. 2418-2421, 2002.

[14] Z. M. Huang, Y. Z. Zhang, M. Kotaki and S.Ramakrishna, "A review on polymer nanofibers by electrospinning and their applications in nanocomposites", *Compos. Sci. Technol.*, vol. 63, no. 15, pp. 2223-2253, 2003.

[15] D. Li and Y. N. Xia, "Electrospinning of nanofibers: Reinventing the wheel?", *Adv. Mater.*, vol. 16, no. 14, pp. 1151-1170, 2004.

[16] S. V. Fridrikh, J. H. Yu, M. P. Brenner and G. C. Rutledge, "Controlling the fiber diameter during electrospinning", *Phys. Rev. Lett.*, vol. 90, no. 14, pp. 144502–144502, 2003.

[17] C. J. Luo, S. D. Stoyanov, E. Stride, E. Pelan and M. Edirisinghe, "Electrospinning versus fibre production methods: From specifics to technological convergence", *Chem. Soc. Rev.*, vol. 41, no. 13, pp. 4708-4735, 2012.

[18] Y. Yamashita, F. Ko, A. Tanaka and H. Miyake, "Characteristics of elastomeric nanofiber membranes produced by electrospinning", *J. Text. Eng.*, vol. 53, no. 4, pp. 137-142, 2007.

[19] S. Paruchuri and M. P. Brenner, "Splitting of a liquid jet", *Phys. Rev. Lett.*, vol. 98, no. 13, pp. 134502-134504, 2007.

[20] G. H. Kim, Y. S. Cho and W. D. Kim, "Stability analysis for multi-jets electrospinning process modified with a cylindrical electrode", *Eur. Polym. J.*, vol. 42, no. 9, pp. 2031-2038, 2006.

[21] Y. Srivastava, M. Marquez and T. Thorsen, "Multijet electrospinning of conducting nanofibers from microfluidic manifolds", *J. Appl. Polymer Sci.*, vol. 106, no. 5, pp. 3171-3178, 2007.

[22] S. A. Theron, A. L. Yarin, E. Zussman and E. Kroll, "Multiple jets in electrospinning: Experiment and modeling", *Polymer*, vol. 46, no. 9, pp. 2889-2899, 2005.

[23] W. Tomaszewski and M. Szadkowski, "Investigation of electrospinning with the use of a multi-jet electrospinning head", *Fibres Text. East. Eur.*, vol. 13, no. 4, pp. 22-26, 2005.

[24] A. Vaseashta, "Controlled formation of multiple Taylor cones in electrospinning process", *Appl. Phys. Lett.*, vol. 90, no. 9, pp. 093115-093115-3, 2007.

[25] A. Varesano, F. Rombaldoni, G. Mazzuchetti, C. Tonin and R. Comotto, "Multi-jet nozzle electrospinning on textile substrates: observations on process and nanofibre mat deposition", *Polym. Int.*, vol. 59, no. 12, pp. 1606-1615, 2010.

[26] S. Xie and Y. Zeng, "Effects of electric field on multineedle electrospinning: Experiment and simulation study", *Ind. Eng. Chem. Res.*, vol. 51, no. 14, pp. 5336-5345, 2012.

[27] A. Varesano, R. A. Carletto and G. Mazzuchetti, "Experimental investigations on the multi-jet electrospinning process", *J. Mater. Proc. Technol.*, vol. 209, no. 11, pp. 5178-5185, 2009.

[28] Y. Yamashita, F. Ko, H. Miyake and Y. Higashiyama, "Establishment of nanofiber preparation technique by electrospinning", *Sen'i Gakkaishi*, vol. 64, no. 1, pp. 24-28, 2008.

[29] A. L. Yarin and E. Zussman, "Upward needleless electrospinning of multiple nanofibers", *Polymer*, vol. 45, no. 9, pp. 2977-2980, 2004.

[30] Y. Liu and J. H. He, "Bubble electrospinning for mass production of nanofibers", *Int. J. Nonlin. Sci. Num. Simul.*, vol. 8, no. 3, pp. 393-396, 2007.

[31] O. O. Dosunmu, G. G. Chase, W. Kataphinan and D. H. Reneker, "Electrospinning of polymer nanofibres from multiple jets on a porous tubular surface", *Nanotechnology*, vol. 17, no. 4, pp. 1123-1127, 2006.

[32] O. Jirsak, P. Sysel, F. Sanetrnik, J. Hruza and J. Chaloupek, "Polyamic acid nanofibers produced by needleless electrospinning", *J. Nanomater.*, vol. 2010, pp. 1-6, 2010.

[33] X. Wang, H. Niu, X. Wang and T. Lin, "Needleless electrospinning of uniform nanofibers using spiral coil spinnerets", *J. Nanomater.*, vol. 2012, pp. 1-9, 2012.

[34] F. L. Zhou, R. H. Gong and I. Porat, "Polymeric nanofibers via flat spinneret electrospinning", *Polym. Eng. Sci.*, vol. 49, no. 12, pp. 2475-2481, 2009.

[35] J. S. Varabhas, G. G. Chase and D. H. Reneker, "Electrospun nanofibers from a porous hollow tube", *Polymer*, vol. 49, no. 19, pp. 4226-4229, 2008.

[36] A. Kumar, M. Wei, C. Barry, J. Chen and J. Mead, "Controlling fiber repulsion in multijet electrospinning for higher throughput", *Macromol. Mater. Eng.*, vol. 295, no. 8, pp. 701-708, 2010.

[37] F. Dabirian, S. A. H. Ravandi and A. R. Pishevar, "Investigation of parameters affecting PAN nanofiber production using electrical and centrifugal forces as a novel method", *Curr. Nanosci.*, vol. 6, pp. 545-552, 2010.

[38] C. T. Peterson, "Hybrid nanomanufacturing process for high-rate polymer nanofiber production", *M.Sc. thesis*, Dept. Mech. & Mater. Eng., University of Nebraska - Lincoln, USA, 2010.

[39] M. R. Badrossamay, H. A. McIlwee, J. A. Goss and K. K. Parker, "Nanofiber assembly by rotary jet-spinning", *Nano. Lett.*,vol. 10, no. 6, pp. 2257-2261, 2010.

[40] K. Sarkar, C. Gomez, S. Zambrano, M. Ramirez, E. de Hoyos, H. Vasquez and K. Lozano, "Electrospinning to forcespinning (TM)", *Mater. Today*, vol. 13, no. 11, pp. 12-14, 2010.

[41] Y. Lu, Y. Li, S. Zhang, G. Xu, K. Fu, H. Lee and X. Zhang, "Parameter study and characterization for polyacrylonitrile nanofibers fabricated via centrifugal spinning process", *Eur. Polym. J.*, vol. 49, no. 12, pp. 3834-3845, 2013.

[42] A. Valipouri, S. A. H. Ravandi and A. R. Pishevar, "A novel method for manufacturing nanofibers", *Fibers Polym.*, vol. 14, no. 6, pp. 941-949, 2013.

[43] I. M. Wallwork, S. P. Decent, A. C. King and R. M. S. M. Schulkes, "The trajectory and stability of a spiralling liquid jet. Part 1. Inviscid theory", *J. Fluid Mech.*, vol. 459, no. 20, pp. 43-65, 2002.

[44] S. P. Decent, A. C. King, M. J. H. Simmons, E. I. Pa˘ra˘u, I. M. Wallwork, C. J. Gurney and J. Uddin, "The trajectory and stability of a spiralling liquid jet: Viscous theory", *Appl. Math. Mod.*, vol. 33, no, 12, pp. 4283-4302, 2009.

[45] E. I. P˘ar˘au, S. P. Decent, M. J. H. Simmons, D. C. Y. Wong and A. C. King, "Nonlinear viscous liquid jets from a rotating orifice", *J. Eng. Math.*, vol. 57, no. 2, pp. 159-179, 2007.